Steady Surface Pressure Measurement via the Lifetime Method with High-Speed Cameras in NASA's Unitary Plan Wind Tunnel

Kenneth R. Lyons*, David D. Murakami†, Marc A. Shaw-Lecerf‡, E. Lara Lash§, Nettie H. Roozeboom¶
NASA Ames Research Center, Moffett Field, CA, 94035

Jie Li‖, Nicholas W. Califano**
Metis Technology Solutions, Inc., Moffett Field, CA 94035

High spatial resolution measurement of steady surface pressure via pressure-sensitive paint at NASA Ames has traditionally relied on specialized cameras equipped to accumulate charge over multiple exposures, whereas measurement of the fluctuating component of pressure uses an altogether separate set of high-speed cameras. To reduce complexity of installation, data acquisition, and processing, we have implemented methods to use a single set of commercial off-the-shelf cameras to produce both steady and unsteady pressure measurements. Both imaging systems were installed in the 11-by 11-foot NASA Ames Unitary Plan Wind Tunnel and acquired images of a scaled model of the Space Launch System Block 1B Crew and Cargo configurations over a variety of flow conditions. This work focuses on methods for data acquisition, processing, and calibration to produce steady-state pressure estimates on the surface of the wind tunnel model based on the lifetime method. It will then compare the steady solutions produced by the legacy and high-speed imaging systems.

Notice to Readers

Certain features and characteristics of the Space Launch System (SLS) vehicle are defined by the U.S. Government as Export-Controlled, Controlled Unclassified Information (CUI). To comply with CUI restrictions, values in some plots and figures have been either removed or normalized to arbitrary values. It is the opinion of the authors that these alternations do not detract from the relevant technical discussions.

I. Introduction

Measurement of steady state pressure levels on wind tunnel models via pressure-sensitive paint (PSP) at NASA Ames has traditionally relied on a specialized set of cameras and legacy software. When fluctuating pressure levels are desired, fast-response paint and a separate set of high-speed cameras are used to measure pressures with high spatial resolution [1, 2]. While steady pressure levels are themselves useful, the steady pressure also determines the gain used in converting intensity to fluctuating pressure in the unsteady processing pipeline. Installation and operation of both optical systems is costly and logistically challenging, particularly in a production environment. As demonstrated previously in a small bench-top wind tunnel test, the same commercial off-the-shelf high-speed cameras used for unsteady PSP may be used to obtain steady pressures using the lifetime method [3]. Here we build on this previous work and present results of acquiring and processing lifetime data using eight Phantom v2512 high-speed cameras, which we call the "high-speed lifetime system", in NASA Ames Research Center's Unitary Plan Wind Tunnel (UPWT) 11-by 11-foot Transonic Wind Tunnel (TWT) as part of the Launch Vehicle Demonstration Test (LVDT). NASA's Space Launch System (SLS) Block 1B Crew and Cargo configurations were installed and tested over a range of Mach numbers, angles of attack, and sideslip angles. Since the same crew configuration model was also used for the 2017 Ascent Unsteady Aerodynamics Test (AUAT) [4], with the legacy lifetime system providing steady surface pressure measurements, steady pressure solutions from that test form a baseline for evaluating the performance of the high-speed system.

*Research Aerospace Engineer, Systems Analysis Office, MS 258–1, AIAA Member
†Research Engineer, Experimental Aero-Physics Branch, MS 260–1
‡Aerospace Engineer, Experimental Aero-Physics Branch, MS 260–1, AIAA Member
§Aerospace Engineer, Experimental Aero-Physics Branch, MS 260–1, AIAA Member
¶Aerospace Engineer, Experimental Aero-Physics Branch, MS 260–1, AIAA Senior Member
‖Senior Research Engineer, Experimental Aero-Physics Branch, MS 260–1
**Software Engineer, Experimental Aero-Physics Branch, MS 260–1

II. Experimental Methods

The 11-by 11-foot UPWT TWT provides a Mach range of 0.2–1.4 and lends itself to optical techniques, with multiple windows in each of its four walls. The 4% SLS Block 1B crew and cargo configurations were used for the test, which is the same model as used in the 2017 AUAT piggyback demonstration [1]. The model was instrumented with 119 Kulite absolute pressure transducers, 176 static pressure ports, and 6 thermocouples. A white base coat was applied to the model, and at the beginning of each test day, porous fast-response paint from Innovative Scientific Solutions, Inc (ISSI) with platinum (pentafluorophenyl) porphyrin (PtTFPP) as the oxygen-sensitive luminophore was applied. While the fast-response paint is not necessarily ideal for measuring steady state pressure, it was chosen to measure high-frequency fluctuations using the high-speed cameras and unsteady processing, as analyzed in companion papers by Shaw-Lecerf et al. [5], Murakami et al. [6], and Li et al. [7]. For more details on the test itself, refer to Lash et al. [8].

Eight Vision Research Phantom v2512 cameras were placed in fore/aft pairs in each of the four tunnel walls. This arrangement emphasized capturing the entire extent of the model rather than maximizing overlapping camera coverage. For runs with the model at zero angle of attack and sideslip, camera resolution was set to 1280×400. Otherwise, the cameras were run at full resolution 1280×800. Forty 400 nm light emitting diode (LED) lamps were also placed in the walls to provide even illumination. The cameras had optical bandpass filters centered at 650 nm to measure only the luminescence of the paint. The lifetime acquisition timing is illustrated in Fig. 1. The lamps were pulsed with a 10 kHz square wave with 50% duty cycle, and camera exposures were triggered to start with the lamp pulses with 45 us exposures.

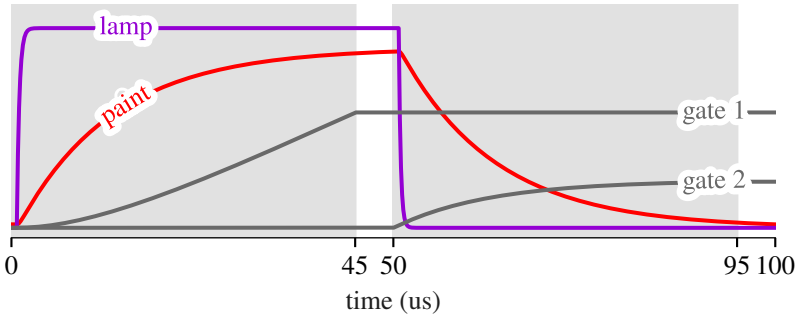

Fig. 1 Lifetime mode data acquisition timing.

In the 2017 AUAT, lifetime PSP measurements were acquired using the same fast-response paint as in LVDT with eight CoolSNAP K4 12-bit cameras (2048×2048 pixels) evenly distributed around the model. The CoolSNAP cameras feature dual output on-chip accumulation to accumulate gate 1 and gate 2 images over multiple exposures.

A. Data Processing

An overview of the processing stages to produce a steady pressure distribution on a 3D grid representation of the wind tunnel model is shown in Fig. 2. The overall processing takes place in three stages: processing images to produce a single gate ratio image for each camera, mapping the images to the 3D grid, and converting the gate ratios on the grid to pressure. Details of the high-speed lifetime processing are discussed below. Note that the processing routines for the legacy system are similar, with most options available in processing steps matched where possible. Processing was performed with a to-be-released version of the `upsp-processing` software (`https://github.com/nasa/upsp-processing`).

1. Image Processing

Due to variations in sensitivities from pixel to pixel in a given camera, each image has flat field correction applied. Flat field images were acquired for each camera using a Gamma Scientific RS–7–1 uniform light source over an evenly spaced sweep of illumination levels from dark to nearly fully saturated. A degree 6 polynomial was fit to the measured response of each pixel versus linearly spaced values from zero to the mean of the brightest image in the sequence, forming the flat field calibration specific to each camera. Each pixel in each image frame is then mapped to the linearized response via the pixel-specific polynomial.

Each image is then registered to the first image in the video to account for motion of the model in the image frame.

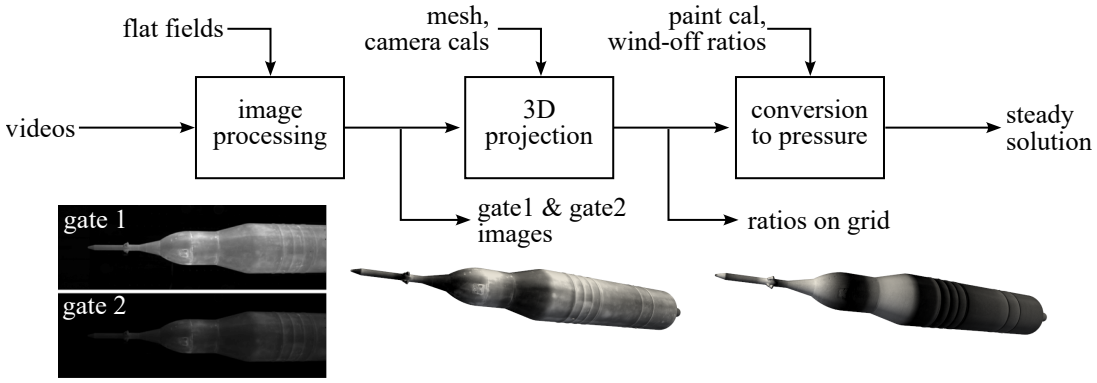

Fig. 2 Data processing overview.

A 2D affine transformation maximizing an enhanced correlation coefficient [9] between image pairs is found and applied with bilinear interpolation sampling. This ability to account for model motion represents a key advantage of the high-speed lifetime system over traditional on-chip accumulation systems for measuring steady pressure, albeit at the expense of high data storage and processing requirements.

The final steps in the image processing stage are: averaging the gate 1 and gate 2 images over time, interpolating over unpainted areas of the model where valid pressure values are desired, and spatially filtering the final images to better match image and 3D grid spatial resolution. In the data presented here, a 3×3 box filter was applied to the averaged gate images.

2. 3D Projection

In order to analyze pressures on the surface of the wind tunnel model, the ratio of gate 2 to gate 1 images in each camera's image plane are mapped to a 3D grid and combined to account for overlapping camera coverage. Overlapping regions are averaged with weights determined by the angle between the vertex normal and the line-of-sight from the vertex to the camera. An initial estimate of the orientations of the cameras and wind tunnel model are based on known tunnel geometry, then the relative orientations between the cameras and model are refined through an external calibration refinement procedure using fiducial markings at known locations on the model and detecting them in the initial frame of the video. Details of this process are described by Califano et al. [10]. Grid vertices are checked for occlusion and are further filtered by checking if the angle between the vertex normal vector and the line-of-sight from the vertex to the camera exceeds 70°. The visible 3D grid vertex positions are mapped into the camera's image plane and pixel values are sampled with bilinear interpolation. The result is a gate ratio at each visible vertex in the surface grid.

3. Conversion to Pressure

Non-uniformity in the measured intensity (or gate ratio) can arise from uneven illumination, variations in model temperature, and uneven paint application. While taking the ratio of gate images reduces the non-uniformity to some extent, it is useful to correct for non-uniformity using wind-off measurements. In this work, we applied an affine correction using a sequence of wind-off measurements over a sweep of static pressures taken at the beginning and end of each day of testing. For each point in the 3D grid, an affine least-squares fit to the measured gate ratio versus the paint calibration is inverted to correct wind-on ratios for non-uniformity.

The lifetime paint calibration used in this work is based on a laboratory calibration fitted to a model of the paint time constant as a function of pressure P and model temperature T:

$$\tau = \frac{\tau_0}{1 + \tau_0 P e^{k_1 + k_2 T}} \tag{1}$$

where τ_0 is the estimated vacuum time constant of the paint and k_1 and k_2 are parameters estimated from laboratory calibration chamber data. Integrals of the exponential paint response over the exposure windows shown in Fig. 1 provide the individual gate values g_1 and g_2. Their ratio can then be calculated over a grid of pressures and temperatures to obtain a paint calibration, shown in Fig. 3, for estimating pressure. An advantage of this paint calibration formulation is that it can flexibly handle varying the data acquisition timing setup without acquiring a new set of calibration chamber

images with those illumination and exposure settings.

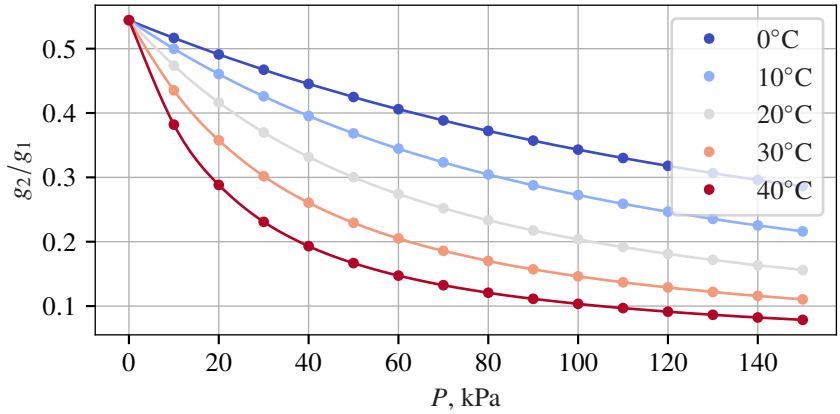

Fig. 3 Model-based lifetime paint calibration.

For the wind-off data used in non-uniformity correction, the expected gate ratio is obtained by interpolating the paint calibration at the average of the thermocouple temperatures and the static pressure from the tunnel data system. For wind-on data, the paint calibration is interpolated at the average thermocouple temperature and the measured gate ratio to compute the pressure at each grid vertex. The pressures are then converted to C_p via the dynamic pressure and free-stream static pressure from the wind tunnel data system. The C_p values from vertices nearby the static pressure taps are then sampled and used to anchor the PSP steady solution. Taps/PSP samples are iteratively culled from the anchoring process if their error is outside two standard deviations of the overall average error. A global offset is then found to minimize the mean square error between remaining pressure taps and paint values.

III. Results

Comparisons between the steady state solution on the 3D grid from the LVDT using the high-speed system and the AUAT using the legacy system are shown in Fig. 4 and Fig. 5. Pressure values are defined at the vertices of a 3D mesh consisting of quadrilateral cells, with interpolation filling the cells to display a smooth surface pressure distribution. All C_p values have been scaled by the same scaler throughout the results. It is important to note that, while the model and wind tunnel between the two test events are identical, only the set Mach number is matched, hence we do not expect perfect agreement. From the perspective shown, most of the data that can be seen is from two cameras with overlap over approximately the middle third of the model length. Some noise may be seen in the high-speed solutions, particularly in the lower-speed condition. Increasing the number of frames processed had negligible impact, indicating that it is not shot noise. Increasing the spatial filter kernel size (e.g. to 5×5) gives a smoother overall solution, but at the expense of spatial resolution. The 3×3 filter size was chosen make the grid and image spatial resolutions approximately equal for most of the model given the camera setup.

Figure 6 gives a comparison between the static pressure tap values and PSP values at nearby grid vertices, arranged spatially in the wind direction. The same vertices were selected between the LVDT and AUAT results, and both solutions were anchored to the static pressure taps via their own global offset, such that the average error should be near zero. As there are multiple pressure taps at or near the same x station circumferentially around the model in some areas, only taps/paint vertices within ±50° azimuth of the surface visible from the perspective in Fig. 4 and 5 are shown. The locations of these taps may be seen in Fig. 5. PSP values are shown as a mean with standard deviation bars. While the direct comparison of the steady pressure on the 3D grid between LVDT and AUAT is confounded by the fact that the tests events were at different times, the static tap values are quite similar between the two tests at this condition. In both the legacy and high-speed data processing systems, some taps are rejected from the offset calculation if the error is out-of-family with the rest, though they are not excluded from the plot. Overall, both the legacy and high-speed systems show similar error levels, with the high-speed system matching better in some locations. The errors tend to be positive at higher (positive) C_p values and negative at lower (negative) C_p values. This is likely due to the use of a single average surface temperature in evaluating the paint calibration to convert from gate ratio to pressure, an assumption both the legacy and high-speed systems currently make.

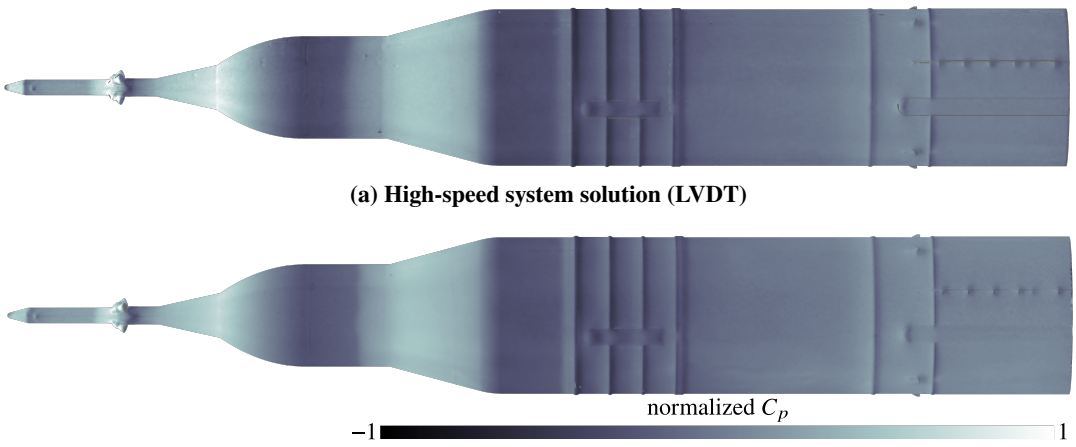

(a) High-speed system solution (LVDT)

(b) Legacy system solution (AUAT)

Fig. 4 Steady state solution at Mach 1.2.

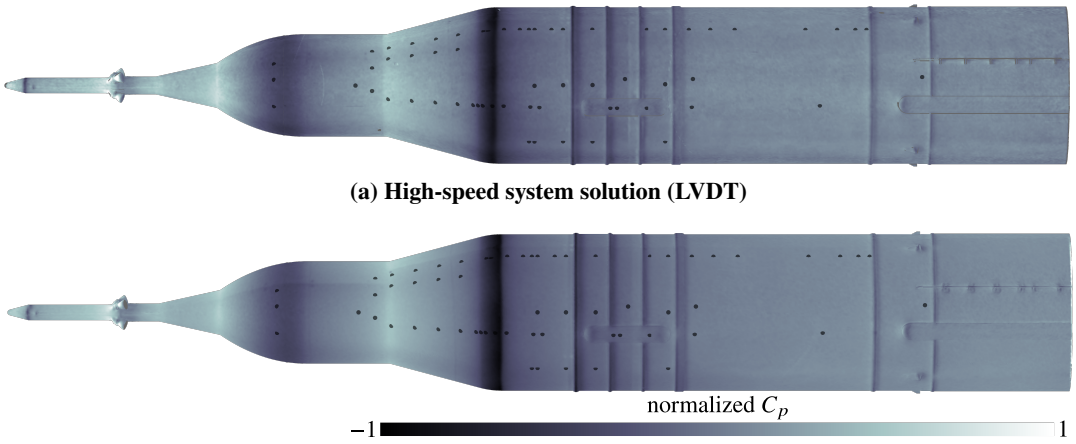

(a) High-speed system solution (LVDT)

(b) Legacy system solution (AUAT)

Fig. 5 Steady state solution at Mach 0.8. Static pressure taps used in Fig. 6 are indicated by black circles.

Figure 7 gives a more comprehensive view of the errors between the PSP and static pressure taps over a coarse Mach sweep, using all taps around the model rather than the limited set in Fig. 6. Kernel density estimates of the error over all PSP-tap samples are shown as a model of the error distribution, with quantiles indicated. Errors are centered around zero with little variation across wind speeds. The error distributions show a slight bimodal quality, particularly with the legacy system, as the comparison in Fig. 6 indicated.

IV. Conclusion

Results from deploying the high-speed lifetime system in the 11-by 11-foot TWT along with associated processing software updates indicate that we can estimate steady state surface pressure with accuracy comparable to the legacy system. This is particularly advantageous logistically when high-resolution unsteady surface pressures are desired, as the single set of cameras can be configured to acquire both lifetime and intensity mode images. The software for processing the data is also set up in a bulk processing pipeline fashion such that the steady solutions from the lifetime system feed directly into unsteady processing. Another key advantage of the high-speed system is acquisition of individual exposures, allowing for accurate localization of surface pressure with model motion.

Future work will include acquiring full-resolution (1280×800) flat field data to handle non-zero angles of attack and

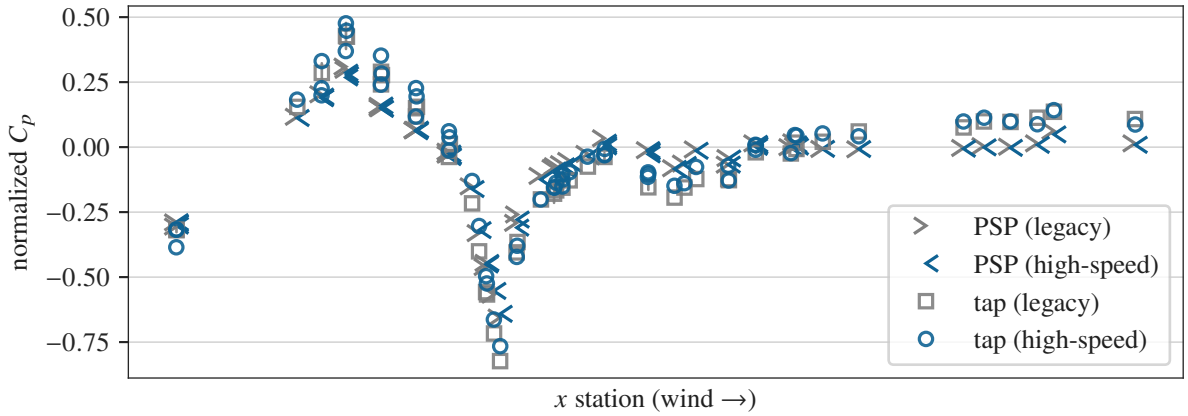

Fig. 6 Paint vs. static tap values along the model at Mach 0.8.

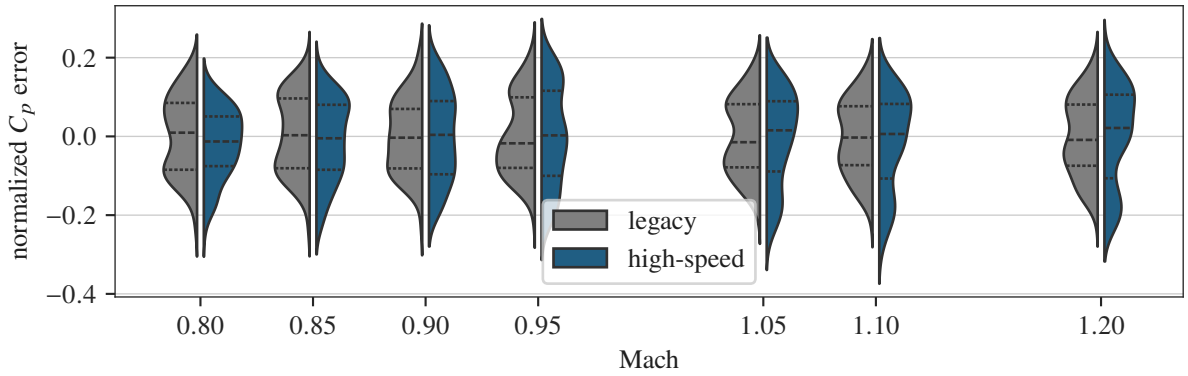

Fig. 7 Kernel density estimates of paint vs. static tap errors over a Mach sweep. Broken lines indicate quartiles.

sideslip. The data will also be re-processed with improvements to the paint calibration process, potentially making greater use of the sequence of wind-off measurements collected at the beginning and end of each day. Finally, it would be interesting to fully characterize the data acquisition system in order to perform optimization studies on the acquisition timing, similar to Yorita et al. [11], accounting for the particular noise characteristics of the high-speed cameras.

Acknowledgments

We would like to thank the NASA Aerosciences Evaluation and Test Capabilities (AETC) portfolio office for funding and supporting this work. We would also like to thank the SLS program for their support of the unsteady PSP technology and the use of the wind tunnel model. Lastly, we would like to thank the staff of the NASA Ames Wind Tunnel Division for their support of unsteady PSP deployment in the TWT.

References

[1] Roozeboom, N. H., Powell, J., Baerny, J. K., Murakami, D. D., Ngo, C. L., Garbeff, T. J., Ross, J. C., and Flach, R., "Development of Unsteady Pressure-Sensitive Paint Application on NASA Space Launch System," *AIAA Aviation 2019 Forum*, Dallas, Texas, 2019. https://doi.org/10.2514/6.2019-3502.

[2] Roozeboom, N. H., Murakami, D. D., Li, J., Shaw-Lecerf, M. A., Lash, E. L., Califano, N. W., Lyons, K. R., Stremel, P. M., Baerny, J. K., Barreras, C. E., Ortega, J. J., and Hand, L. A., "NASA's Unsteady Pressure-Sensitive Paint Research and Operational Capability Developments," *AIAA SciTech Forum*, National Harbor, MD, 2023. https://doi.org/10.2514/6.2023-0636.

[3] Murakami, D. D., Shaw-Lecerf, M. A., Lash, E. L., Lyons, K. R., and Roozeboom, N. H., "Implementation of the

Lifetime Method in Unsteady Pressure Sensitive Paint Measurements," *AIAA SciTech Forum*, National Harbor, MD, 2023. https://doi.org/10.2514/6.2023-0635.

[4] Steva, T. B., Pollard, V. J., Herron, A., and Crosby, W. A., "Space Launch System Aeroacoustic Wind Tunnel Test Results," *AIAA Aviation 2019 Forum*, American Institute of Aeronautics and Astronautics, 2019. https://doi.org/10.2514/6.2019-3303.

[5] Shaw-Lecerf, M. A., Lash, E. L., Lyons, K. R., Murakami, D. D., Roozeboom, N. H., Li, J., and Califano, N., "Spatiotemporal Analysis of High-Resolution Pressure-Sensitive Paint Measurements on a Launch Vehicle Wind Tunnel Model," *AIAA SCITECH 2025 Forum*, American Institute of Aeronautics and Astronautics, 2025.

[6] Murakami, D. D., Hand, L. A., Lyons, K. R., Shaw-Lecerf, M. A., Lash, E. L., Califano, N., and Li, J., "Error Estimation for Unsteady Pressure Sensitive Paint Measurements," *AIAA SCITECH 2025 Forum*, American Institute of Aeronautics and Astronautics, 2025.

[7] Li, J., Lyons, K. R., Lash, E. L., Roozeboom, N., Shaw-Lecerf, M. A., Murakami, D. D., and Califano, N. W., "Spectral Proper Orthogonal Decomposition of uPSP Measurements in Recent NASA Ames Wind Tunnel Test," *AIAA SCITECH 2025 Forum*, American Institute of Aeronautics and Astronautics, 2025.

[8] Lash, E. L., Murakami, D. D., Shaw-Lecerf, M. A., Lyons, K. R., Li, J., Califano, N. W., Crowe, E., and Roozeboom, N., "uPSP Launch Vehicle DemonstrationTest at NASA Ames Research Center," *AIAA SCITECH 2025 Forum*, American Institute of Aeronautics and Astronautics, 2025.

[9] Evangelidis, G., and Psarakis, E., "Parametric Image Alignment Using Enhanced Correlation Coefficient Maximization," *IEEE Transactions on Pattern Analysis and Machine Intelligence*, Vol. 30, No. 10, 2008, pp. 1858–1865. https://doi.org/10.1109/tpami.2008.113.

[10] Califano, N., Shaw-Lecerf, M., and Roozeboom, N., "Unsteady Pressure Sensitive Paint Camera Calibration Improvements," *AIAA SCITECH 2023 Forum*, American Institute of Aeronautics and Astronautics, 2023. https://doi.org/10.2514/6.2023-2447.

[11] Yorita, D., Henne, U., and Klein, C., "Improvement of Lifetime-based PSP Technique for Industrial Wind Tunnel Tests," *55th AIAA Aerospace Sciences Meeting*, American Institute of Aeronautics and Astronautics, 2017. https://doi.org/10.2514/6.2017-0703.